

1 Wastewater SARS-CoV-2 RNA Concentration and Loading Variability from Grab  
2 and 24-Hour Composite Samples

3

4 Kyle Curtis, David Keeling, Kathleen Yetka, Allison Larson, Raul Gonzalez\*

5 Hampton Roads Sanitation District, 1434 Air Rail Avenue, Virginia Beach, VA 23455

6

7 \*Corresponding author email: [rgonzalez@hrsd.com](mailto:rgonzalez@hrsd.com)

8

9 Keywords

10 SARS-CoV-2

11 Wastewater epidemiology

12 Composite sampling

13 Viral load

14

15 Abstract

16 The ongoing COVID-19 pandemic caused by severe acute respiratory syndrome coronavirus 2 (SARS-  
17 CoV-2) requires a significant, coordinated public health response. Assessing case density and spread of  
18 infection is critical and relies largely on clinical testing data. However, clinical testing suffers from

19 known limitations, including test availability and a bias towards enumerating only symptomatic  
20 individuals. Wastewater-based epidemiology (WBE) has gained widespread support as a potential  
21 complement to clinical testing for assessing COVID-19 infections at the community scale. The efficacy of  
22 WBE hinges on the ability to accurately characterize SARS-CoV-2 RNA concentrations in wastewater. To  
23 date, a variety of sampling schemes have been used without consensus around the appropriateness of  
24 grab or composite sampling. Here we address a key WBE knowledge gap by examining the variability of  
25 SARS-CoV-2 RNA concentrations in wastewater grab samples collected every 2 hours for 72 hours  
26 compared with three corresponding 24-hour flow-weighted composite samples collected over the same  
27 period. Results show relatively low variability (respective means for N1, N2, N3 assays = 608, 847.9,  
28 768.4 copies 100 mL<sup>-1</sup>, standard deviations = 501.4, 500.3, 505.8 copies 100 mL<sup>-1</sup>) for grab sample  
29 concentrations, and good agreement between most grab samples and their respective composite (mean  
30 deviation from composite = 159 copies 100 mL<sup>-1</sup>). When SARS-CoV-2 RNA concentrations are used to  
31 calculate viral load (RNA concentration \* total influent flow the sample day), the discrepancy between  
32 grabs (log<sub>10</sub> range for all grabs = 11.9) or a grab and its associated 24-hour composite (log<sub>10</sub> difference =  
33 11.6) are amplified. A similar effect is seen when estimating carrier prevalence in a catchment  
34 population with median estimates based on grabs ranging 63-1885 carriers. Findings suggest that grab  
35 samples may be sufficient to characterize SARS-CoV-2 RNA concentrations, but additional calculations  
36 using these data may be sensitive to grab sample variability and warrant the use of flow-weighted  
37 composite sampling. These data inform future WBE work by helping determine the most appropriate  
38 sampling scheme and facilitate sharing of datasets between studies via consistent methodology.

39

40

41

## 42 1. Introduction

43 The outbreak of the novel severe acute respiratory syndrome coronavirus 2 (SARS-CoV-2) in late 2019  
44 escalated to a global pandemic. To date (11-2-2020) there are over 46.7 million confirmed cases and 1.2  
45 million deaths world-wide attributed to COVID-19, the disease caused by SARS-CoV-2 (Dong et al.,  
46 2020). Understanding the extent and density of infection is critical in effectively responding to this  
47 pandemic. However, due to limited diagnostic testing (Babiker et al., 2020, Schneider 2020) and  
48 inconsistent reporting of results (Leonor, 2020), generating reliable COVID-19 prevalence estimates in a  
49 community remains challenging. This is compounded by asymptomatic disease transmission, the rate of  
50 which is still unclear (Kronbichler et al., 2020).

51 Wastewater-based epidemiology (WBE) represents a promising complement to clinical testing as a  
52 means of assessing COVID-19 trends and prevalence within a community. WBE has been used to  
53 investigate occurrence and trends for a variety of chemical (pharmaceuticals, illicit drugs) and biological  
54 (pathogens, antibiotic resistance genes) constituents at the community-scale by measuring biomarkers  
55 in wastewater (Choi et al., 2018, Been et al., 2014, Sims and Ksprzyk-Hordern, 2020). Unlike clinical  
56 testing data, which is limited by test availability and biased towards the detection of symptomatic  
57 individuals, WBE yields a community-scale viral load estimate for a wastewater treatment facility's  
58 catchment population. Considering these benefits, there has been much support for WBE as a  
59 complementary strategy to clinical testing in response to the SARS-CoV-2 pandemic (Ahmed et al., 2020,  
60 Bivins et al., 2020, Hata et al., 2020).

61 The use of WBE in a variety of geographically and demographically disparate areas creates the  
62 opportunity to coordinate efforts, assimilate data, and assess SARS-CoV-2 trends on a larger scale than  
63 any single WBE study could alone. For this broad, integrated approach to succeed many knowledge  
64 gaps must first be addressed for appropriate data comparisons. Such areas include sample collection,

65 preservation, concentration, and quantification in a complex and challenging wastewater matrix (Bivins  
66 et al., 2020, Daughton, 2020, Kitajima et al., 2020, Mao et al., 2020, Worley-Morse et al., 2019). A  
67 fundamental study design knowledge gap considers how to collect a sample that is appropriately  
68 representative of SARS-CoV-2 concentrations in wastewater. Given that influent flows at wastewater  
69 facilities fluctuate continually it is important to understand if these variations in flow correspond to  
70 significant virus concentration variation. Specifically, do grab samples sufficiently characterize  
71 wastewater SARS-CoV-2 concentrations, or are flow-weighted composites necessary?

72 We address this knowledge gap via a comparison of grab and 24-hr flow-weighted composite samples  
73 over a 3-day intensive time series. The goal was to characterize SARS-CoV-2 variability in grab samples  
74 collected every 2hrs for 72 hours and compare this variability with 3 flow-weighted composites collected  
75 over the same time frame. Specific objectives are; 1) to examine the variability of reverse transcription  
76 droplet digital PCR (RT-ddPCR) quantified SARS-CoV-2 RNA concentrations, 2) compare daily loading  
77 calculations from grab sample concentrations with loading calculations using respective 24-hr flow-  
78 weighted composite concentrations, and 3) compare carrier prevalence estimates from grab sample  
79 concentrations with carrier prevalence estimates using respective 24-hr flow-weighted composite  
80 concentrations.

81 This work will aid future WBE studies in determining the most appropriate sampling scheme. Increasing  
82 the chance of accurately characterizing SARS-CoV-2 concentrations in wastewater allows WBE work to  
83 provide the best available data for use in subsequent calculations, such as estimates of community  
84 infections or epidemiological models.

85

86 **2. Methods**

87 *2.1 Wastewater Treatment Facility*

88 Army Base Treatment Plant (ABTP) is in Norfolk, VA, and is operated by Hampton Roads Sanitation  
89 District (HRSD). It services an area of approximately 21 square miles, which is dominated by residential  
90 development, a port, and a large military base. The treatment plant serves a population of  
91 approximately 78,322, however this figure can fluctuate considerably due to the arrival and departure of  
92 military vessels and cargo ships. The catchment population can also vary based on redirection of flow  
93 throughout the collection system, a practice that is common for wastewater utilities.

94 For ABTP, pretreatment involves coarse screening via bar screens. Residual suspended solids, fats, oils,  
95 and grease are removed during a primary settling step. Secondary treatment consists of a 5-stage  
96 Bardenpho system and secondary settling. Secondary clarifier effluent is disinfected with sodium  
97 hypochlorite and dechlorinated via sodium bisulfite prior to discharge. ABTP has a design flow of 68  
98 million liters per day with a peak capacity of 136 million liters per day, and average daily flows ranging  
99 38-42 million liters per day. Over the three-day study period, the average daily flow was 47.2 million  
100 liters per day.

101 *2.2 Study Design*

102 Samples were aseptically collected over a 72-hour period (5/1/2020 10:00 EST– 5/4/2020 10:00 EST)  
103 from the ABTP Raw Water Influent (RWI) sample point prior to pretreatment. Thirty-six uniform 1L grab  
104 samples were collected every two hours using an ISCO Avalanche portable refrigerated sampler  
105 (Teledyne ISCO, Lincoln, NE) which kept the samples at approximately 4°C. For each of 3, 24-hour  
106 periods, a flow-weighted composite sample was collected concurrently with the sequentially collected  
107 grabs using an ISCO 3710 Portable sampler (Teledyne ISCO). The composite sampler was paced to take a  
108 150mL aliquot every 870,550 liters, with all aliquots collected in a sterile 15L carboy in a sampler base  
109 filled with ice that was replenished daily. Final Effluent (FNE) samples were collected aseptically after

110 the 30-minute chlorine contact point between mid-morning and mid-day of each collection. Each set of  
111 24-hour composite samples were transported on ice from the sampling site to the HRSD Central  
112 Environmental Laboratory (within 4 hours) where samples were processed upon arrival.

### 113 *2.3 Sample Processing*

114 Electronegative filtration, following the method in Worley-Morse et al. (2019), was used to concentrate  
115 SARS-CoV-2 from 50 mL of raw wastewater and 200 mL of treated final effluent. Filters were stored in a -  
116 80°C freezer immediately after concentration until RNA extraction using the NucliSENS easyMag  
117 (bioMerieux Inc., Durham, NC, USA) modified protocol described in Worley-Morse et al. Prior to  
118 extraction,  $1 \times 10^7$  copies of Hep G Armored RNA (Asuragen, Austin, TX, USA) was spiked in the lysis  
119 buffer for all samples and negative extraction controls to quantify matrix inhibition. One-step RT-ddPCR  
120 was used to enumerate SARS-CoV-2 N1, N2, and N3 assays (Lu et al., 2020) and the Hep G inhibition  
121 control on a Bio-Rad QX200 (Bio-Rad, Hercules, CA, USA) using the protocol in Gonzalez et al (2020).  
122 Inhibition was determined by calculating the Hep G recovery in the samples compared to the NEC.  
123 Samples were not re-run when inhibition was an issue (less than 10% recovery). A detailed RT-ddPCR  
124 protocol and run summary statistics can be found in the Supplemental Information.

### 125 *2.4 Estimating SARS-CoV-2 Infections in the Sewage Collection System*

126 A promising extension of WBE is calculating prevalence estimates to better gauge the number of  
127 infected individuals (both symptomatic and asymptomatic) in a community. This approach has been  
128 used in several recent SARS-CoV-2 publications (Ahmed et al., 2020, Medema et al., 2020, Wu et al.,  
129 2020). The number of SARS-CoV-2 infected carriers for the ABTP service area were estimated using two  
130 values—viral load per person and total viral load to the treatment facility. For the purpose of viral load  
131 and carrier prevalence estimates, only the N2 assay was used. N2 was selected based on superior  
132 performance in previous work (Gonzalez et al. 2020), assessed by frequency of detection in wastewater.

133 Equation 1 was used to calculate the viral load per person (the total amount of virus shed by an infected  
134 person via feces). The 90<sup>th</sup> percentile concentration of SARS-CoV-2 in stool reported from Wölfel et al.  
135 (2020) was used as variable A in equation 1. A triangular distribution (minimum= 51, likeliest= 128,  
136 maximum= 796) for the fecal mass per person per day, variable B, was fitted from Rose et al. (2015).  
137 This distribution was sampled during each of 10,000 Monte Carlo simulations conducted using Oracle  
138 Crystal Ball (Oracle, Berkshire, UK).

139 Equation 1.

$$Load_{indiv} = C_{indiv} \times m$$

140

141 where;

142  $Load_{indiv}$  = Viral load per person (copies day<sup>-1</sup>)

143  $C_{indiv}$  = concentration of SARS-CoV-2 virus in feces (copies g<sup>-1</sup>)

144  $m$  = typical mass of stool produced per person per day (g day<sup>-1</sup>)

145 Total viral load to the WWTP during each sampling event was calculated using equation 2. In order to  
146 quantify potential carriers in the population the N2 assay concentration for each sample was used as the  
147  $C_{WWTP}$  value in Equation 2.

148 Equation 2.

$$Load_{WWTP} = C_{WWTP} \times Q \times f$$

150 where;

151  $Load_{WWTP}$  = Viral load to WWTP (copies day<sup>-1</sup>)

152  $C_{WWTP}$  = concentration of SARS-CoV-2 in wastewater samples (copies 100 mL<sup>-1</sup>)

153  $Q$  = Plant flow (million liters per day, million liters day<sup>-1</sup>)

154  $f$  = Conversion factor between 100 mL and million liters day<sup>-1</sup>

155

156 Prevalence estimates were calculated using equation 3, which incorporated results from equations 1

157 and 2 for each sampling event.

158 Equation 3.

159 
$$I = \frac{Load_{WWTP}}{Load_{indiv}}$$

160

161

162 where;

163  $I$  = Estimated proportion of WWTP service area infected

164

## 165 *2.5 Data Analysis and Visualization*

166 Data analysis and visualization was conducted using R Statistical Computing Software version 3.6.3. (R

167 Core Team, 2019). The dplyr (Wickham et al., 2015) and tidyr (Wickham et al., 2018) packages were

168 primarily used for data manipulation and the ggplot2 package (Wickham 2016) was used for all plotting.

169 The code used to create each figure can be found at

170 [https://github.com/mkc9953/WW\\_EPI\\_grab\\_composite\\_study](https://github.com/mkc9953/WW_EPI_grab_composite_study).

171

172 3. Results and Discussion

173 Three large wastewater facilities collect and treat portions of the city of Norfolk's wastewater. The ABTP  
174 currently receives wastewater from approximately 36% of the city's population. During the study period  
175 there was 211, 211, and 239 cumulative clinically confirmed COVID-19 cases in the entire city (for days  
176 1, 2, and 3, respectively). Gonzalez et al. (2020) have been monitoring this facility, amongst others,  
177 weekly since March 9<sup>th</sup>, 2020. Detections of SARS-CoV-2 began on April 6, 2020—4 weeks prior to this  
178 study.

179 *3.1 Influent Flow and Rainfall*

180 Hourly wastewater influent flow during the study period ranged from 27.1 to 61.6 million liters per day,  
181 with a mean flow of 46.6 million liters per day and standard deviation of 103 million liters per day. A  
182 description of flow characteristics by sample day can be found in Table 1. Two days prior to the first  
183 sampling event there was a storm generating approximately 2.5 cm of rainfall. A brief increase in flow  
184 was observed, likely due to stormwater infiltrating the sewer collection system. Influent flow at the  
185 treatment facility returned to typical dry weather values in approximately 6hrs and remained at levels  
186 typical of dry weather throughout the study. No rainfall occurred in the vicinity of the treatment facility  
187 during the study period. The treatment facility serves several low-lying areas that are subject to  
188 inundation during moderate high tide events, causing saltwater intrusion into sewer collection system.  
189 Treatment plant influent conductivity, used as an indicator of seawater, begins to increase significantly  
190 following tidal levels greater than 1.07 meters Mean Lower Low Water (MLLW). High tides during the  
191 period sampled were 1.04 meters MLLW or less based on the Sewell's Point Tide Gage operated by  
192 NOAA.

193 *3.2 SARS-CoV-2 Concentration and Variability*

194 All three assays used for this study (N1, N2, N3) yielded positive results for every raw wastewater  
195 influent sample. All three final effluent samples were below the limit of detection (LOD = 24, 40, and 30  
196 copies 100 mL<sup>-1</sup> for N1, N2, and N3 assays, respectively). For composite samples, concentrations of all  
197 assays ranged from 580 – 1380 copies 100 mL<sup>-1</sup>, with a mean of 900 and standard deviation of 215  
198 copies 100 mL<sup>-1</sup>, showing good agreement across the three days (Figure 1). Similarly, composite samples  
199 showed relatively low variability within (largest range = 490 copies 100 mL<sup>-1</sup>) and between assays  
200 (largest range = 580 copies 100 mL<sup>-1</sup>) for a given day (Table 2). Grab sample concentration variability  
201 was also low, ranging from 25 to 1100 copies 100 mL<sup>-1</sup> for all samples collected (Table 3) with a  
202 coefficient of variation (CV) of 68.5%. Grab sample concentrations showed good agreement across  
203 assays as means, minima, and maxima were each in the same respective order of magnitude (Table 3).  
204 Examining the association between each pair of assays showed a positive monotonic relationship for all  
205 combinations, with Spearman coefficients ranging 0.72-0.90 (Figure 2). Comparing results by day for all  
206 assays showed similarly low variability with the greatest difference in any two daily mean  
207 concentrations of 114.8 copies 100 mL<sup>-1</sup> (Table 3).

208 Grab sample concentrations showed good agreement with corresponding composite concentrations  
209 (Figure 1), with a mean deviation of 159 copies 100 mL<sup>-1</sup> between a grab sample and its associated  
210 composite. Over half (55%) of the total number of grab samples (59/108) had concentrations which  
211 were within 50% of their respective composite. The discrepancy between grab and composite  
212 concentrations, regardless of magnitude, showed grabs at lower concentration than the corresponding  
213 composite for 69% of samples (75/108) (Figure 1). These drops in virus concentration were not  
214 concurrent with times of lowest influent flow but seemed to lag by approximately 4-6hrs (Figure 1). This  
215 pattern may be influenced by the number and density of COVID-19 infections in the region. In a case  
216 with few infected individuals the viral signal would be sporadic in the daily flow. Conversely, if a  
217 catchment area were highly impacted by infections, the virus signal in wastewater would be less variable

218 and minimally influenced by changes in flow. The ABTP catchment could have a high enough infection  
219 density to consistently detect a wastewater signal, but not so ubiquitous that the signal is entirely  
220 unimpacted by diurnal cycles in flow. Additionally, the grab samples with the extreme low  
221 concentrations were affected most by inhibition. For example, the sample with the lowest concentration  
222 ( $N_1 = 50$  copies  $100\text{mL}^{-1}$ ) had a Hep G recovery (0.19%) approximately 2 orders of magnitude less than  
223 the meansample recovery (17%). It is possible that times of low flow have more concentrated matrix  
224 inhibitors that affect PCR more severely, thus underrepresenting concentrations. Considering this, grab  
225 samples should be collected at times that avoid early morning flow minima (e.g. 0800-1100) and the  
226 subsequent 4-6hrs dips in viral concentration, in order to reduce the likelihood of underestimating viral  
227 load to the treatment facility.

### 228 *3.3 Viral Load and Carrier Prevalence*

229 Wastewater N2 SARS-CoV-2 concentrations were used to calculate viral load for grab and composite  
230 samples (Figure 3). Viral loads calculated using composite sample values showed low variability between  
231 days, ranging from  $4.2 \times 10^{11}$  –  $6.3 \times 10^{11}$  copies  $\text{day}^{-1}$ . Variability in daily load derived using grab sample  
232 concentrations was greater, ranging from  $4.2 \times 10^{10}$  –  $9.3 \times 10^{11}$  copies  $\text{day}^{-1}$ , with a mean of  $4.0 \times 10^{11}$   
233 copies  $\text{day}^{-1}$  and standard deviation of  $2.3 \times 10^{11}$  copies  $\text{day}^{-1}$ . While the variability in grab sample  
234 concentration (CV=68.5%) and viral load calculated from grab sample concentration (CV=58.4%) are  
235 expectedly similar, the magnitude of any given deviation in viral load is increased due to the way load is  
236 derived (Equation 2). For example, the greatest difference in concentration between a grab and  
237 composite sample, within a common assay, was 1340 copies  $100 \text{ mL}^{-1}$ . When viral load is calculated  
238 using this same grab and composite the difference between the two types of sample is  $4.1 \times 10^{11}$  copies  
239  $\text{day}^{-1}$ . For all load calculations using grab sample values, the mean deviation from the corresponding  
240 composite value was  $9.3 \times 10^{10}$  copies  $\text{day}^{-1}$ , or 16.6%. Data presented here demonstrate the large

241 disparity in viral load values calculated using SARS-CoV-2 concentrations given a difference in only 2hrs  
242 between grab sample collection times. For this study grab samples more often had lower  
243 concentrations than the corresponding composite, thus there is a higher likelihood of underestimating  
244 concentrations when collecting grabs. Viral concentration data which are biased low will affect  
245 downstream calculations made using these data, such as estimates of viral load and carrier prevalence in  
246 the catchment population. If these metrics are used to inform a public health response it is critical that  
247 they do not systematically underestimate the extent of COVID-19 infections in the community.

248

249 SAR-CoV-2 concentrations in wastewater can also be used to estimate the prevalence of carriers in a  
250 catchment population (Equation 3). Currently there is considerable uncertainty around the viral  
251 shedding rate in feces of people infected with COVID-19. A widely reference paper by Wölfel et al.  
252 (2020) examining nine clinical cases found concentrations of SARS-CoV-2 viral RNA in stool ranging from  
253 below the limit of detection ( $100 \text{ copies g}^{-1}$ ) to  $7.1 \times 10^8 \text{ copies g}^{-1}$ . Furthermore, sensitivity analysis of a  
254 previous carrier prevalence model highlights the high susceptibility to the shedding rate variability,  
255 increasing the error associated with resulting estimates. However, as viral shedding rate is more fully  
256 described, carrier estimates could become increasingly important, given the potential public health  
257 value in generating a reliable estimate of changes in infection rates in a catchment. Results of this study  
258 highlight the importance of collecting a sample that is representative of SARS-CoV-2 concentrations in  
259 wastewater, as subsequent viral load and carrier estimates are based on this value. As with viral  
260 concentration and viral load data, variability was low in carrier estimates for composite samples with  
261 median values of 714, 1074, 720 infected individuals (Figure 3). When including the 10<sup>th</sup> and 90<sup>th</sup>  
262 percentile results, estimates ranged from 369 to 2511 carriers in the catchment as estimated from  
263 composite samples. Carrier estimates based on grab samples were more variable, with 10<sup>th</sup> to 90<sup>th</sup>

264 percentile model estimates ranging from 33 to 4408 carriers, and median estimates ranging from 63-  
265 1855 carriers. The median carrier estimate from 23 of 36 grab samples fell within the 10<sup>th</sup>-90<sup>th</sup>  
266 percentile range for the corresponding composite. Of the 13 grabs for which the median carrier  
267 estimate was outside of the composite estimate 10<sup>th</sup> – 90<sup>th</sup> range, 12 were below the composite  
268 estimate range. Because these calculations are based on viral concentration it was expected that  
269 estimates from grabs would more often be lower than estimates made using composite concentrations.  
270 For these data, the potential underestimation of median carrier prevalence due to collecting a grab  
271 sample rather than a composite could be as large as 1011 people, based on the minimum median carrier  
272 estimate (63) and corresponding composite estimate (1074) (Figure 3). That discrepancy in estimated  
273 carriers has practical implications if WBE is used as a component of the public health response to the  
274 SARS-CoV-2 pandemic. Choosing an appropriate sampling scheme can minimize potential bias  
275 introduced into these estimates by accurately characterizing viral concentration. If replication in other  
276 studies shows that grab samples reliably underestimate viral concentration, then either composite  
277 sampling or grab samples targeting the expected peak viral concentration should be employed to reduce  
278 the likelihood of generating data which are biased low.

279

### 280 *3.4 Limitations and Future Work*

281 One important consideration for using WBE to examine viral trends during a pandemic is the  
282 heterogenous and dynamic nature of the spread of infections. Epidemiological work has shown that,  
283 particularly during the early stages of pathogen spread, rates of infection are not uniform but rather  
284 clustered in localized hotspots often driven by importation of cases (Bajardi et al., 2009) and the  
285 disproportionate effects of “superspreading” events (Lipsitch, et al., 2003). Interpreting WBE data is  
286 also confounded by transient use of the sewerage system from people who may be infected but do not

287 live in the catchment area, e.g. tourists or people who commute to a different area for work.  
288 Restrictions such as stay-at-home orders and the subsequent reopening of cities add further complexity  
289 to the characteristics of viral spread in a community. As a result, extrapolation of findings from one  
290 catchment to the surrounding region are not often appropriate. Therefore, data and patterns presented  
291 here pertain to this specific catchment over a 3-day period, and do not easily extend to other areas or  
292 timeframes. To address this, we suggest a surveillance approach to WBE, monitoring multiple  
293 catchments on a routine basis to characterize trends specific to a region over time. As noted, variability  
294 in influent concentration change as density of cases increase or decrease within the catchment.  
295 Calculations using influent flow, such as viral load and carrier prevalence, will also be influenced by daily  
296 and seasonal changes in influent flow volume as well as short term increases due to wet weather.  
297 Regular monitoring of facilities reduces some uncertainty by establishing a context for changes in viral  
298 loading. Though estimating carrier prevalence remains challenging due to uncertainty around viral  
299 shedding rates, tracking viral load from a catchment over time may be sufficient to gain insight into  
300 community-level trends.

301

302

#### 303 4. Conclusions

- 304 - SARS-CoV-2 concentration variability in wastewater was low (CV=68.5%) for grab samples  
305 collected every 2 hours for 72 hours
- 306 - The three CDC recommended assays (N1, N2, N3) were highly correlated, with the strongest  
307 association observed between N2 and N3 (Spearman's rho = 0.9)

- 308 - Grab samples showed good agreement with corresponding 24hr flow-weighted composites  
309 collected from the same period (mean deviation = 159 copies 100 mL<sup>-1</sup> between a grab sample  
310 and its associated composite)
- 311 - Discrepancies between grab samples and associated composite are scaled-up when data are  
312 used to estimate viral load and carrier prevalence
- 313 - Grab sample concentrations were lower than their respective composite for 69% (75/108) of  
314 samples, suggesting the possibility of introducing a bias towards lower concentration when  
315 using grabs

316

317

318

## 319 References

- 320 1. Ahmed, W., Angel, N., Edson, J., Bibby, K., Bivins, A., O'Brien, J.W., Choi, P.M., Kitajima, M.,  
321 Simpson, S.L., Li, J. and Tscharke, B.. First confirmed detection of SARS-CoV-2 in untreated  
322 wastewater in Australia: A proof of concept for the wastewater surveillance of COVID-19 in the  
323 community. *Sci. Total Environ.* 2020, (728) 138764.
- 324
- 325 2. Babiker, A.; Myers, C.W.; Hill, C.E.; Guarner, J. SARS-CoV2-2 Testing: Trials and Tribulations. *Am. J. of*  
326 *Clin. Pathol.* 2020, (153) 706-708

327

328

- 329 3. Bajardi, P.; Poletto, C.; Ramasco, J.J.; Tizzoni, M.; Colizza, V.; Vespignani, A. Human Mobility  
330 Networks, Travel Restrictions, and the Global Spread of 2009 H1N1 Pandemic. *PLoS One*. 2011b,  
331 6(1).  
332
- 333 4. Been, F.; Rossi, L.; Ort, C.; Rudaz, S.; Delémont, O.; Esseiva, P. Population normalization with  
334 ammonium in wastewater-based epidemiology: Application to illicit drug monitoring. *Environ. Sci.*  
335 *Technol.* 2014, 48(14), 8162-8169.  
336  
337
- 338 5. Bivins A.; .... Bibby, K. Wastewater-Based Epidemiology: Global Collaborative to Maximize  
339 Contributions in the Fight Against COVID-19. *Environ. Sci. Technol.* 2020, DOI:  
340 10.1021/acs.est.0c02388.  
341
- 342 6. Lu, X., Wang, L., Sakthivel, S.K., Whitaker, B., Murray, J., Kamili, S., Lynch, B., Malapati, L., Burke,  
343 S.A., Harcourt, J. and Tamin, A., 2020. US CDC real-time reverse transcription PCR panel for  
344 detection of severe acute respiratory syndrome coronavirus 2. *Emerging infectious diseases*, 26(8),  
345 p.1654.  
346  
347
- 348 7. Choi, P.M.; Tschärke, B.J.; Donner, E.; O'Brien, J.W.; Grant, S.C.; Kaserzon, S.L.; Mackie, R.; O'Malley,  
349 E.; Crosbie, N.D.; Thomas, K.V; Mueller, J.F. Wastewater-based epidemiology biomarkers: past,  
350 present and future. *Trend. Anal. Chem.* 2018, (105) 453-469.  
351
- 352 8. Daughton, C. The international imperative to rapidly and inexpensively monitor community-wide  
353 COVID-19 infection status and trends. *Sci. Total Environ.* 2020, (726) 138149  
354

- 355
- 356 9. Dong, E.; Du, H.; Gardner, L. An Interactive Web-Based Dashboard to Track COVID-19 in Real  
357 Time. *Lancet Infect. Dis.* 2020, 3099 (20), 19– 20, DOI: 10.1016/S1473-3099(20)30120-1  
358
- 359 10. Gonzalez, R.; Curtis, K.; Bivins, A.; Bibby, K.; Weir, M.; Yetka, K.; Thompson, H.; Keeling, D.; Mitchell,  
360 J.; Gonzalez, D. COVID-19 Surveillance in Southeastern Virginia Using Wastewater -Based  
361 Epidemiology. *Water. Res.* 2020, (186), 116296.  
362  
363
- 364 11. Hata, A.; Honda, R. Potential Sensitivity of Wastewater Monitoring for SARS-CoV-2: Comparison with  
365 Norovirus Cases. *Environ. Sci. Technol.* 2020, DOI: 10.1021/acs.est.0c02271.  
366
- 367 12. Leonor, M. Virginia Misses Key Marks on Virus Testing and Leaders Eye Reopening. Richmond  
368 Times-Dispatch. [https://www.richmond.com/special-report/coronavirus/virginia-misses-key-marks-  
369 on-virus-testing-as-leaders-eye-reopening/article\\_021e12c6-6d20-5030-9068-4caaeda495f7.html](https://www.richmond.com/special-report/coronavirus/virginia-misses-key-marks-on-virus-testing-as-leaders-eye-reopening/article_021e12c6-6d20-5030-9068-4caaeda495f7.html)  
370  
371
- 372 13. Kitajima, M.; Ahmed, W.; Bibby, K.; Carducci, A.; Gerba, C.P.; Hamilton, K.A.; Harmoto, E.; Rose, J.B.  
373 SARS-CoV-2 in wastewater: State of the knowledge and reasearch needs. *Sci. Total Environ.* 2020,  
374 (739) 139076.  
375
- 376 14. Kronbichler, A.; Kresse, D.; Yoon, S.; Lee, K.W.; Effenberger, M.; Shin, J.I. Asymptomatic patients as a  
377 source of COVID-19 infections: A systematic review and meta-analysis. *Int. J. Infect. Dis.* 2020, In  
378 Press. DOI: 10.1016/j.ijid.2020.06.052  
379

380

381 15. Lipsitch, M.; Cohen, T.; Cooper, B.; Robins, J.M.; Ma, S.; James, J.; Gopalakrishna, G.; Chew S.K.; Tan,  
382 C.C.; Samore, M.H., Fisman, D.; Murray, M. Transmission Dynamics and Control of Severe Acute  
383 Respiratory Disease. *Science*. 2003, (300) 1966-1970.

384

385 16. Mao, K.; Zhang, K.; Du, W.; Ali, W.; Feng, X.; Zhang, H. The potential of wastewater-based  
386 epidemiology as surveillance and early warning of infectious disease outbreaks. *Curr. Opin. Environ.*  
387 *Sci. Health*. 2020, (17), 1-7.

388

389

390 17. Medema, G.; Heijnen, L.; Elsinga, G.; Italiaander, R.; Brouwer, A. Presence of SARS-Coronavirus-2 in  
391 Sewage and Correlation with Reported COVID-19 Prevalence in the Early Stage of the Epidemic in  
392 the Netherlands. *Environ. Sci. Technol. Lett.* 2020, DOI: 10.1021/acs.estlett.0c00357

393

394 18. R Core Team (2017). R: A language and environment for statistical computing. R Foundation for  
395 Statistical Computing, Vienna, Austria. URL <https://www.R-project.org/>.

396

397

398 19. Rose, C.; Parker, A.; Jefferson, B.; Cartmell, E. The Characterization of Feces and Urine: A Review of  
399 the Literature to Inform Advanced Treatment Technology. *Crit. Rev. Environ. Sci. Technol.* 2015, (45)  
400 1827-1879.

401

402 20. Schneider, E.C. Failing the Test- The Tragic Data Gap Undermining the U.S. Pandemic Response. *N.*  
403 *Engl. J. Med.* 2020, DOI: 10.1056/NEJMp2014836

404

405

406 21. Sims, N.; Kasprzyk-Hordern, B. Future perspectives of wastewater-based epidemiology: Monitoring  
407 infectious disease spread and resistance to the community level. *Environ. Int.* 2020, (139), DOI:  
408 10.1016/j.envint.2020.105689.

409

410 22. Wickham, H. *ggplot2: elegant graphics for data analysis*. Springer-Verlag New York. 2016, ISBN 978-  
411 3-319-24277-4, <https://ggplot2.tidyverse.org>.

412

413

414 23. Wickham, H.; Francois, R.; Henry, L; Müller, K. *dplyr: A grammar of data manipulation*. R package  
415 version 0.8.5. 2015. <https://CRAN.R-project.org/package=dplyr>

416

417 24. Wickham, H.; Henry, L. *tidyr: Easily Tidy Data with 'spread()' and 'gather()' Functions*. R package  
418 version 1.0.2. 2018 <https://CRAN.R-project.org/package=tidyr>

419

420

421 25. Wölfel R.; Corman, V.M.; Guggemos, W.; Seilmaier, M.; Zange, S.; Muller, M.A.; Niemeyer, D.; Jones,  
422 T.C.; Vollmar, P.; Camilla, R.; Hoelscher, M.; Bleicker T.; Brunink, S.; Schneider, J.; Ehmann, R.;  
423 Zwirgmaier, K.; Drosten, C.; Wendtner, C. Virological assessment of hospitalized patients with  
424 COVID-19. *Nature*. 2020, (581) 465-469

425

426 26. Worley-Morse, T.; Mann, M.; Khunjar, W.; Olabode, L.; Gonzalez, R. Evaluating the fate of bacterial  
427 indicators, viral indicators, and viruses in wastewater resource recovery facilities. *Water Environ.*  
428 *Res.* 2019, (91) 830-842.

429

430

431 27. Wu, F.; Xiao, A.; Zhang, J.; Gu, X.; Lee, W.L.; Kauffman, K.; Hanage, W.; Matus, M.; Ghaeli, N.; Endo,

432 N.; Duvallet, C.; Moniz, K.; Erickson, T.; Chai, P.; Thompson, J.; Alm, E. SARS-CoV-2 titers in

433 wastewater are higher than expected from clinically confirmed cases. medRxiv, 2020. doi:

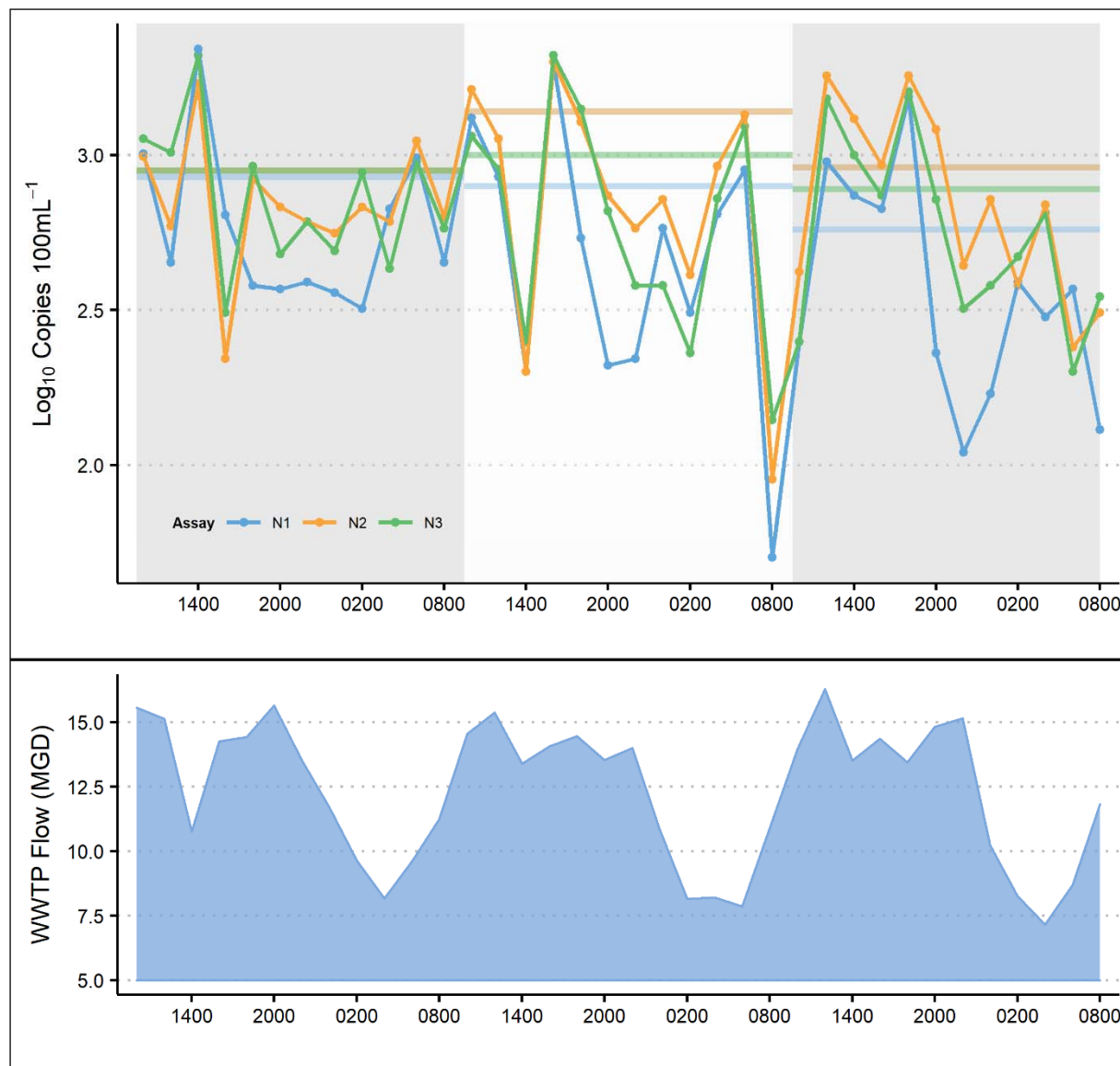
434 <https://doi.org/10.1101/2020.04.05.20051540>

435

436

437

438 Figure 1.



439

440

441 Figure 1 Caption.

442 Wastewater  $\text{log}_{10}$  SARS-CoV-2 concentrations (copies  $100\text{ mL}^{-1}$ ). Grab sample concentrations are

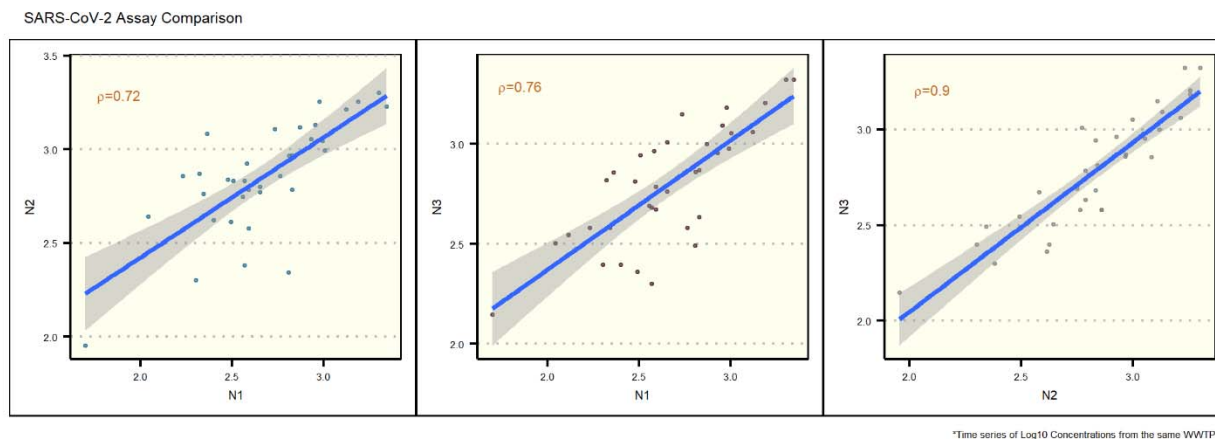
443 denoted by dots with each color representing an assay (N1, N2, N3). Grey and white shaded areas

444 denote the timeframe for three discrete 24hr flow-weighted composites. Horizontal lines denote

445 concentrations for each composite sample. Influent flow is plotted in the lower panel.

446

447 Figure 2.



448

449

450

451 Figure 2 Caption.

452 Associations between SARS-CoV-2 assays (N1, N2, N3). X and Y axes show  $\log_{10}$  concentrations for each

453 assay. Lines represent linear associations between assays, shaded areas denote standard error for each

454 regression line. Spearman correlation coefficients are listed in orange on each plot.

455

456

457

458

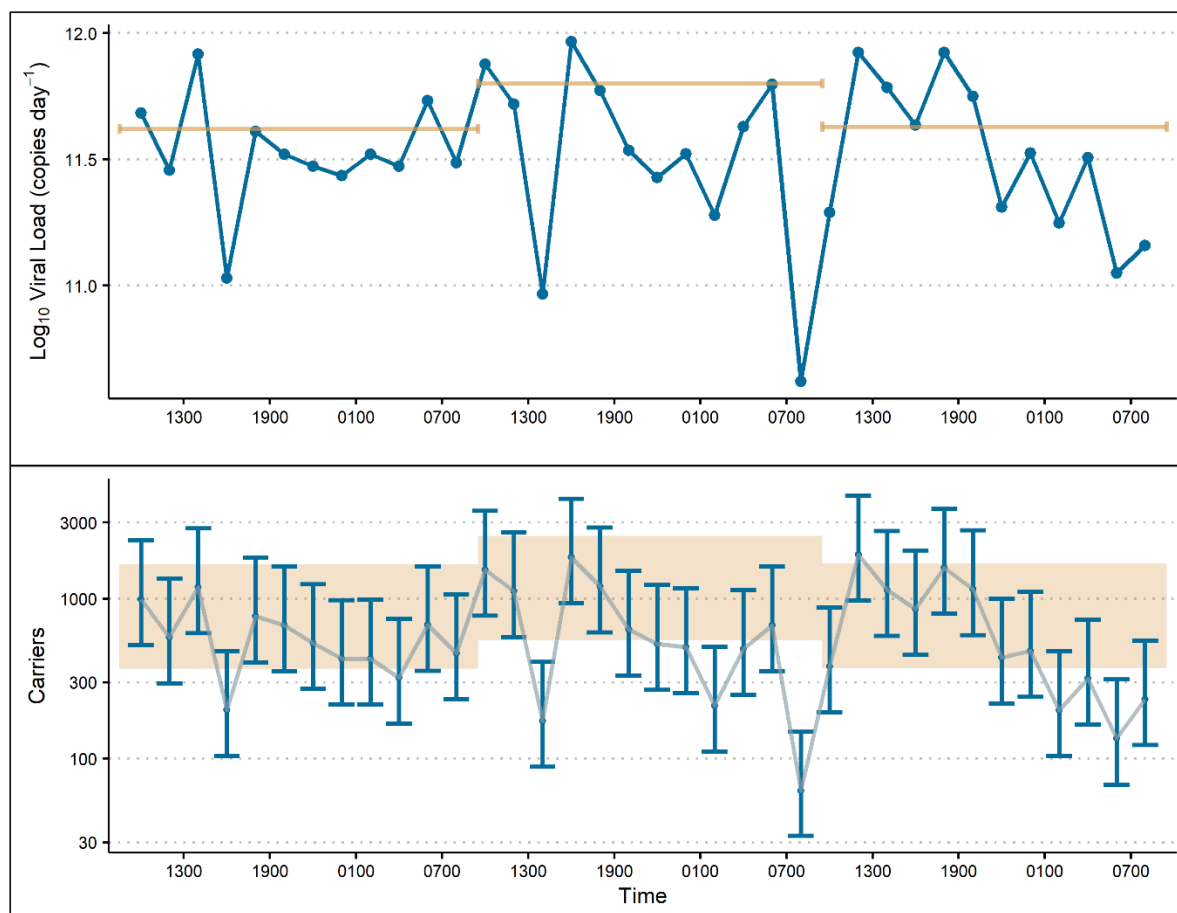
459

460

461

462

463 Figure 3



464

465 Figure 3 Caption.

466 Wastewater SARS-CoV-2 load and carrier prevalence estimates for the 72-hour study period. For the  
467 upper panel, load ( $\log_{10}$  copies) calculated using grab sample concentrations are denoted by blue dots  
468 while load from 24-hour composite concentrations are denoted by horizontal orange lines. In the lower  
469 panel, prevalence of SARS-CoV-2 infected carriers is estimated using Monte Carlo simulation. Estimates  
470 derived using grab sample concentrations are denote by blue dots (median number of carriers per  
471 simulation) with error bars indicating the 10<sup>th</sup> and 90<sup>th</sup> percentile range in estimates. Shaded areas  
472 indicate the 10<sup>th</sup> and 90<sup>th</sup> percentile range of carrier estimates calculated using 24-hour composite  
473 samples.

474 Table 1.

Influent Flow For Study Period (Million Liters per Day)					
	Min	Max	Mean	Standard Deviation	Hour of Peak flow
Day 1	31.0	59.2	47.2	9.8	2000
Day 2	29.8	58.2	45.8	10.5	1200
Day 3	27.1	61.6	46.6	11.4	1200

475

476

477 Table 1 Caption.

478 Wastewater influent flow characteristics for each of the three days during which samples were

479 collected.

480

481

482

483

484

485

486

487

488 Table 2.

SARS-CoV-2 Composite Sample Concentration (copies 100mL <sup>-1</sup> )				
Date	Composite	N1	N2	N3
5/2/2020	1	860	890	890
5/3/2020	2	800	1380	1010
5/4/2020	3	580	910	780

489

490 Table 2 Caption.

491 SARS-CoV-2 RNA concentrations for each 24-hour, flow-weighted composite sample by assay.

492

493

494

495

496

497

498

499

500

501

502 Table 3.

SARS-CoV-2 Grab Sample Concentration (copies 100 mL <sup>-1</sup> )				
By Assay				
	N1	N2	N3	Overall
Min	50	90	140	50
Max	2200	2000	2100	1100
Mean	608	848	768	741
St. Dev	501	500	506	508
By Day				
	Day 1	Day 2	Day 3	Overall
Min	220	50	110	50
Max	2200	2100	1800	1100
Mean	759	790	675	726
St. Dev	456	571	497	502

503

504 Table 3 Caption.

505 SARS-CoV-2 grab sample RNA concentration descriptive statistics by assay and sample day.

506

507

508

509

510

511

